

Isobutane Cracking over Y-Zeolites

II. Catalytic Cycles and Reaction Selectivity

G. Yaluris,* J. E. Rekoske,* L. M. Aparicio,* R. J. Madon,^{†,1} and J. A. Dumesic*¹

*Center for Clean Industrial and Treatment Technologies, Department of Chemical Engineering, University of Wisconsin, Madison, Wisconsin 53706; and [†]Engelhard Corporation, 101 Wood Avenue, Iselin, New Jersey, 08830

Received July 15, 1994; revised December 19, 1994

We describe the activity and selectivity of isobutane cracking on Y-zeolite-based catalysts in terms of catalytic cycles composed of initiation, β -scission, oligomerization, olefin desorption, isomerization, and hydride ion transfer reactions involving carbenium ions. Olefin desorption and isomerization reactions are at quasi-equilibrium, with the former reactions determining the surface carbenium ion coverages. Microcalorimetric measurements of ammonia adsorption show that catalyst steaming leads to a decrease in the number and strength of acid sites. Decreasing the strength of Brønsted acid sites results in decreasing surface carbenium ion coverages and decreasing rates of all reactions. The hydride ion transfer cycles are affected most by catalyst steaming, leading to lower paraffin selectivities. Lower temperatures and higher conversions increase carbenium ion coverages and favor hydride ion transfer cycles, leading to higher paraffin selectivities. © 1995 Academic Press, Inc.

Press, Inc.

tion, isomerization, and hydride ion transfer reactions. These reactions were sufficient for obtaining rates of formation of all major products, distribution of C₃, C₄, and C₅ hydrocarbons, and selectivity to paraffins and olefins. This model effectively described observed changes in catalyst performance with conversion, temperature, and catalyst steaming. In this paper, we use the kinetic model to quantitatively analyze the catalytic cycles that occur during catalytic cracking and to address the role of different catalytic cycles in determining the activity and selectivity of the catalyst. We also address how factors such as conversion, temperature, and acid strength affect the rates of reactions that make up these catalytic cycles, and discuss relationships between these factors and catalyst performance.

INTRODUCTION

Over the last several years, many researchers (1-9) have investigated reactions of small (C₄, C₅) hydrocarbons on solid acid catalysts. Significant discussion has centered on the process for carbenium ion initiation and its role in hydrocarbon cracking. Justifiably, small molecules are chosen to allow one to readily identify and investigate individual steps in an otherwise complex reaction scheme. Even the cracking of a molecule as small as isobutane requires a large number of reaction steps to describe the major observed products (8, 9). An understanding of how these individual steps are related is essential to explain the overall cracking process.

In our first paper (10), we developed a kinetic model for isobutane cracking over Y-zeolite-based fluid catalytic cracking (FCC) catalysts using the principles of carbonium and carbenium ion chemistry. The model included important reactions that take place during catalytic cracking: initiation, β -scission, oligomerization, olefin desorp-

EXPERIMENTAL

In Ref. (10), we gave a detailed description of the experimental procedures used to collect kinetic data for isobutane cracking over two Y-based FCC catalysts, and summarized the preparation and properties of the catalysts. One catalyst, USY-C, was calcined at 840 K for 2 h, and the other catalyst, USY-S, was calcined and then steamed for 2 h at 1060 K.

Using an apparatus described in Ref. (11), we determined the distribution of acid site strengths for the USY-C and USY-S catalysts from microcalorimetric measurements of differential heats of ammonia adsorption at 423 K. Catalyst samples (100-500 mg) were loaded into quartz cells and evacuated for 1 h at room temperature. The temperature was subsequently raised to 573 K, and the samples were evacuated for 1 h. The catalyst was then calcined at 723 K for 2 h in 500 Torr of static oxygen. During this treatment, oxygen was periodically added to and evacuated from the cells. The samples were evacuated again at 723 K for 1.5 h and cooled to room temperature. The calorimeter block was positioned around the cells and the samples were finally evacuated overnight at 423 K. Small doses (ca. 1-5 μ mol) of ammonia were then

¹ To whom correspondence should be addressed.

admitted sequentially into the cells at 423 K, and the differential heats of adsorption were obtained versus coverage (12).

RESULTS

Figure 1 shows differential heats of ammonia adsorption versus coverage on USY-C and USY-S catalysts. It is obvious from the figure that acid sites on USY-C are stronger than those on USY-S. Figure 2 shows histograms of acid site strength distributions for USY-C and USY-S catalysts. We obtained these histograms by first fitting data of differential heats of adsorption versus coverage by a polynomial and then using the fitted polynomial to determine the amount of adsorbed NH_3 within a given range of differential heats. These results show that when the catalyst is steamed, the acid site strength distribution shifts toward weaker sites. The relative number of sites that adsorb NH_3 with a differential heat of about 130 kJ/mol is reduced by about 60%, while the relative number of stronger sites is also reduced. The sites that increase after steaming are weaker ones that adsorb NH_3 with a differential heat of about 110 kJ/mol and lower. We have shown by infrared spectroscopic studies of pyridine adsorption (10, 13) that steaming reduces the number of Brønsted acid sites more than the number of Lewis acid sites. Thus, steaming results in the preferential loss of Brønsted acid sites corresponding to NH_3 adsorption with a differential heat of about 130 kJ/mol. This conclusion agrees with earlier work (13) indicating that the sites of intermediate strength in Y-zeolites are predominantly Brønsted acids, and their number and strength are reduced with steaming.

We gave details of the activation energies and preexponential factors of the individual reaction steps used in the kinetic model for isobutane cracking over USY-C and USY-S catalysts in Ref.(10). Tables 1 and 2 give the forward and net turnover frequencies (TOF) for these steps. Table 1 shows rates for USY-C at the reactor entrance

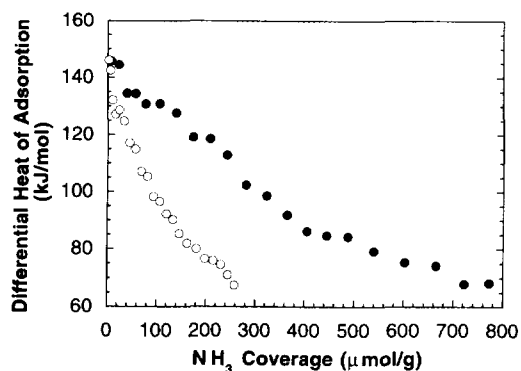


FIG. 1. Differential heats of ammonia adsorption on USY-C (●) and USY-S (○) at 423 K.

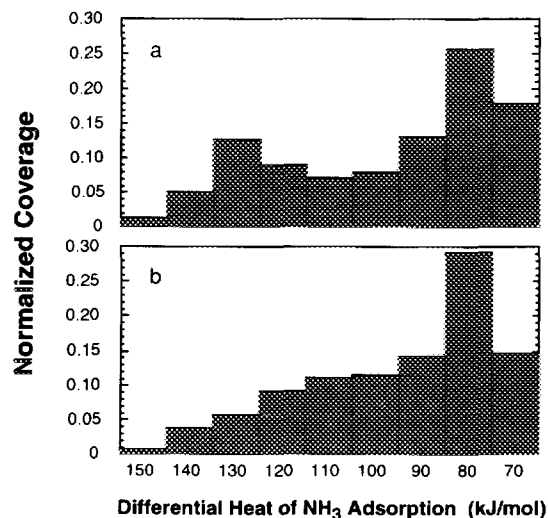


FIG. 2. Acid site strength distributions from NH_3 microcalorimetry at 423 K for catalysts (a) USY-C and (b) USY-S. Coverage normalized with respect to the total number of acid sites for each catalyst.

TABLE 1
Turnover Frequencies (s^{-1}) of Individual Reaction Steps for Isobutane Cracking on USY-C at 773 K (11% Conversion) at Reactor Inlet and Outlet

	Catalyst USY-C, 11% conversion			
	Reactor entrance (Conversion 0.2%)		Reactor outlet (Conversion 11%)	
	Forward rate (s^{-1})	Net rate (s^{-1})	Forward rate (s^{-1})	Net rate (s^{-1})
Step 1	1.2×10^{-3}	1.2×10^{-3}	8.1×10^{-4}	8.1×10^{-4}
Step 2	2.1×10^{-3}	2.1×10^{-3}	1.4×10^{-3}	1.4×10^{-3}
Step 3	1.3×10^{-6}	1.3×10^{-6}	4.7×10^{-4}	4.7×10^{-4}
Step 4	4.6×10^4	1.5×10^{-3}	4.6×10^5	-3.2×10^{-3}
Step 5	1.3×10^{-5}	1.2×10^{-5}	4.3×10^{-3}	3.4×10^{-3}
Step 6	6.3×10^{-3}	1.2×10^{-5}	1.5×10^1	3.4×10^{-3}
Step 7	1.8×10^{-5}	1.2×10^{-5}	4.4×10^{-2}	3.4×10^{-3}
Step 8	6.8×10^{-8}	5.2×10^{-8}	8.1×10^{-4}	7.5×10^{-4}
Step 9	1.2×10^{-4}	5.2×10^{-8}	4.6×10^{-1}	7.5×10^{-4}
Step 10	3.4×10^{-7}	5.2×10^{-8}	1.3×10^{-3}	7.5×10^{-4}
Step 11	2.0×10^2	5.2×10^{-8}	2.9×10^4	7.5×10^{-4}
Step 12	2.5×10^{-4}	5.2×10^{-8}	3.5×10^{-2}	7.5×10^{-4}
Step 13	1.0×10^4	8.4×10^{-4}	1.6×10^5	4.6×10^{-3}
Step 14	3.6×10^6	1.5×10^{-3}	5.6×10^7	6.7×10^{-3}
Step 15	2.2×10^3	2.3×10^{-4}	3.5×10^4	1.5×10^{-4}
Step 16	1.3×10^4	4.5×10^{-4}	2.0×10^5	2.8×10^{-4}
Step 17	1.0×10^4	3.0×10^{-4}	1.6×10^5	1.9×10^{-4}
Step 18	1.1×10^2	6.7×10^{-6}	6.2×10^4	1.1×10^{-4}
Step 19	5.9×10^{-4}	5.9×10^{-4}	5.4×10^{-3}	5.3×10^{-3}
Step 20	4.4×10^{-4}	4.4×10^{-4}	6.2×10^{-3}	6.0×10^{-3}
Step 21	6.0×10^{-6}	6.0×10^{-6}	3.0×10^{-3}	2.6×10^{-3}

Note. The reaction steps are given in Fig. 1 of Ref. (10).

TABLE 2

Turnover Frequencies (s^{-1}) of Individual Reaction Steps for Isobutane Cracking at Reactor Outlet on Catalyst USY-C at 773 K (11 and 40% Conversions) and at 733 K (12% Conversion), and on USY-S at 773 K (10% Conversion)

Catalyst:	USY-C		USY-C		USY-C		USY-S	
Temperature (K):	773		773		733		773	
Pressure (kPa):	151.7		122.8		125.2		137.3	
Conversion (%):	11.2		40.5		12.4		10.0	
	Forward rate (s^{-1})	Net rate (s^{-1})	Forward rate (s^{-1})	Net rate (s^{-1})	Forward rate (s^{-1})	Net rate (s^{-1})	Forward rate (s^{-1})	Net rate (s^{-1})
Step 1	8.1×10^{-4}	8.1×10^{-4}	3.8×10^{-4}	3.8×10^{-4}	1.3×10^{-4}	1.3×10^{-4}	6.8×10^{-4}	6.8×10^{-4}
Step 2	1.4×10^{-3}	1.4×10^{-3}	6.4×10^{-4}	6.4×10^{-4}	2.3×10^{-4}	2.3×10^{-4}	6.6×10^{-4}	6.6×10^{-4}
Step 3	4.7×10^{-4}	4.7×10^{-4}	9.8×10^{-4}	9.8×10^{-4}	6.6×10^{-5}	6.6×10^{-5}	1.6×10^{-4}	1.6×10^{-4}
Step 4	4.6×10^5	-3.2×10^{-3}	1.1×10^6	-5.0×10^{-3}	1.7×10^5	-1.4×10^{-3}	6.5×10^5	-7.3×10^{-4}
Step 5	4.3×10^{-3}	3.4×10^{-3}	8.1×10^{-3}	3.5×10^{-3}	1.5×10^{-3}	1.2×10^{-3}	1.5×10^{-3}	1.3×10^{-3}
Step 6	1.5×10^1	3.4×10^{-3}	8.5×10^1	3.5×10^{-3}	1.2×10^1	1.2×10^{-3}	4.7	1.3×10^{-3}
Step 7	4.4×10^{-2}	3.4×10^{-3}	2.4×10^{-1}	3.5×10^{-3}	1.7×10^{-2}	1.2×10^{-3}	1.3×10^{-2}	1.3×10^{-3}
Step 8	8.1×10^{-4}	7.5×10^{-4}	2.4×10^{-3}	1.8×10^{-3}	2.6×10^{-4}	2.4×10^{-4}	2.3×10^{-4}	2.1×10^{-4}
Step 9	4.6×10^{-1}	7.5×10^{-4}	5.0	1.8×10^{-3}	3.5×10^{-1}	2.4×10^{-4}	1.6×10^{-1}	2.1×10^{-4}
Step 10	1.3×10^{-3}	7.5×10^{-4}	1.4×10^{-2}	1.8×10^{-3}	4.8×10^{-4}	2.4×10^{-4}	4.7×10^{-4}	2.1×10^{-4}
Step 11	2.9×10^4	7.5×10^{-4}	2.1×10^5	1.8×10^{-3}	2.5×10^4	2.4×10^{-4}	1.2×10^4	2.1×10^{-4}
Step 12	3.5×10^{-2}	7.5×10^{-4}	2.5×10^{-1}	1.8×10^{-3}	9.9×10^{-3}	2.4×10^{-4}	1.5×10^{-2}	2.1×10^{-4}
Step 13	1.6×10^5	4.6×10^{-3}	2.1×10^5	5.5×10^{-3}	7.1×10^4	1.6×10^{-3}	2.1×10^5	1.7×10^{-3}
Step 14	5.6×10^7	6.7×10^{-3}	7.2×10^7	4.5×10^{-3}	4.8×10^7	2.5×10^{-3}	1.9×10^7	2.5×10^{-3}
Step 15	3.5×10^4	1.5×10^{-4}	4.4×10^4	9.2×10^{-5}	1.3×10^4	2.8×10^{-5}	4.4×10^4	7.3×10^{-5}
Step 16	2.0×10^5	2.8×10^{-4}	2.6×10^5	1.7×10^{-4}	8.5×10^4	5.7×10^{-5}	2.6×10^5	1.4×10^{-4}
Step 17	1.6×10^5	1.9×10^{-4}	2.0×10^5	1.2×10^{-4}	6.4×10^4	3.8×10^{-5}	2.0×10^5	9.1×10^{-5}
Step 18	6.2×10^4	1.1×10^{-4}	1.2×10^5	8.9×10^{-5}	2.5×10^4	2.4×10^{-5}	6.1×10^4	4.6×10^{-5}
Step 19	5.4×10^{-3}	5.3×10^{-3}	7.6×10^{-3}	7.5×10^{-3}	1.9×10^{-3}	1.9×10^{-3}	1.6×10^{-3}	1.6×10^{-3}
Step 20	6.2×10^{-3}	6.0×10^{-3}	4.5×10^{-3}	4.1×10^{-3}	2.5×10^{-3}	2.4×10^{-3}	2.2×10^{-3}	2.2×10^{-3}
Step 21	3.0×10^{-3}	2.6×10^{-3}	3.4×10^{-3}	1.7×10^{-3}	1.3×10^{-3}	9.8×10^{-4}	1.2×10^{-3}	1.0×10^{-3}

Note. The reaction steps are given in Fig. 1 of Ref. (10).

and exit. Table 2 compares rates on USY-C (i) at 11 and 40% conversions, (ii) at 773 K and 733 K, with (iii) rates on USY-S at 773 K. Pressure differences for the experiments are small and are accounted for in the model. Therefore, we can make comparisons of reaction rates for different catalysts and reaction conditions.

The model showed (10) that the key kinetic parameter that differed between USY-C and USY-S was ΔH_+ , the heat of stabilization of a carbenium ion relative to the heat of stabilization of a proton on the catalyst. The value of ΔH_+ increased by 2 kcal/mol for the steamed catalyst. Higher values of this parameter indicate a decreased ability of the catalyst to stabilize carbenium ions on the surface, and thus indicate a catalyst with lower Brønsted acid strength. The increase in ΔH_+ with steaming suggests that such treatment causes not only a decrease in the number of acid sites but leads to a decrease in the acid strength. This result from the model is substantiated as described above by our microcalorimetric measurements. The lower strength of the Brønsted acid sites due to steaming is reflected by a change in the catalytic activity per acid site: the site time yield for isobutane conversion is

reduced from $0.011 s^{-1}$ for catalyst USY-C to $0.005 s^{-1}$ for catalyst USY-S (at 10–11% conversion and 773 K). This agrees with earlier results (14, 15) that indicated changes in acid strength to be a factor in cracking activity of zeolites with Na^+ or NH_4^+ exchange. Also, as Brønsted acid strength decreases, fractional carbenium ion coverages on USY-S decrease (Table 3). Changes in coverage have a direct effect on selectivity. For example, as the Brønsted acid strength decreases for USY-S the olefin selectivity increases over that for USY-C: the paraffin to olefin ratio at 11% conversion is 2.6 for USY-C compared to 1.6 for USY-S.


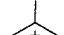
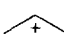


Fractional Surface Coverages

Fractional surface coverages obtained here from microkinetic modeling are comparative and not absolute (10). Thus, it is possible to compare coverages on different catalysts or at different experimental conditions.

Conversion. Figure 3 shows changes of propyl, isobutyl, and isopentyl carbenium ion coverages with reactor length (or conversion). Isobutyl cation coverage increases

TABLE 3

Surface Coverages of the Most Abundant Species at the Reactor Outlet for Catalyst USY-C at 773 and 733 K and Catalyst USY-S at 773 K

Species	USY-C		USY-S
	773 K, 152 kPa	773 K, 125 kPa	773 K, 137 kPa
H ⁺	7.3×10^{-1}	5.8×10^{-1}	9.1×10^{-1}
	1.9×10^{-5}	1.5×10^{-5}	7.2×10^{-6}
	2.1×10^{-1}	3.3×10^{-1}	6.9×10^{-2}
	5.7×10^{-6}	4.9×10^{-6}	1.9×10^{-6}
	6.3×10^{-2}	9.4×10^{-2}	1.7×10^{-2}
	4.8×10^{-4}	7.8×10^{-4}	1.9×10^{-4}

Note. Conversion equal to 10–12%.

at low conversions, but the rate of increase is lower at higher conversions as oligomerization reactions become significant and consume these species. Coverage by isopentyl cations increases more gradually at low conversions because it is formed by secondary processes, i.e., oligomerization/ β -scission reactions. The rate of increase of the isopentyl cation coverage is even more gradual at high conversions since it can also be consumed by these same processes. Propyl cation coverage initially increases with conversion in a manner similar to the isobutyl cation. These species are also formed by oligomerization/ β -scission reactions; at higher conversions, increased rates of these reactions lead to further increases in propyl carbenium ion coverage.

Temperature. Since olefin desorption reactions are endothermic, decreasing the temperature increases the

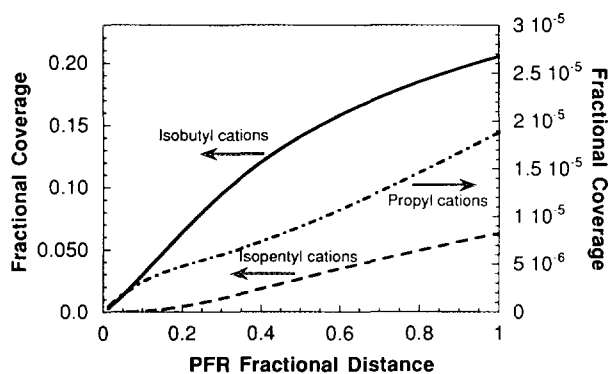


FIG. 3. Surface coverages of propyl (---), isobutyl (—), and isopentyl (· · ·) carbenium ions versus reactor length for catalyst USY-C at 773 K and 11% conversion.

total surface coverage by carbenium ions (Table 3). This effect more than compensates for the decrease in surface coverages that one would expect because of the decrease in the gas phase olefin partial pressure due to lower olefin selectivity at lower temperatures. The increase in surface coverage is due to increases in the coverages of tertiary carbenium ions. Since isomerization of tertiary to secondary carbenium ions is also endothermic, lower temperatures favor the formation of tertiary carbenium ions, and coverages of secondary carbenium ions decrease slightly at lower temperatures. The importance of the quasi-equilibrated olefin adsorption/desorption step for determining carbenium ion surface coverages will be discussed in detail later.

Steaming. The higher value of ΔH_{+} for the steamed catalyst leads to lower coverages by carbenium ions. As would be predicted for a weaker acid, proton coverage for USY-S is higher than for USY-C. Table 3 shows the fractional surface coverages of the most abundant species predicted by the model for USY-C and USY-S catalysts at the outlet of the plug-flow reactor at ca. 10–12% conversion. The most abundant surface carbenium ion is the isobutyl cation followed by the isopentyl cation. The decrease in Brønsted acid strength by steaming decreases carbenium ion coverages by about a factor of 3. This occurs even though the steamed catalyst shows an increased selectivity for olefin production and the partial pressure of olefins is higher.

The rate constant of the ethylene production step is reduced by a factor of 2 with steaming (10). This reaction is thought to take place on electron acceptor sites, which could be Lewis acid sites. Therefore, this result suggests a decrease in the acid strength of these sites with steaming, in agreement with earlier microcalorimetric results (13).

DISCUSSION

Catalytic Cycles

Catalytic cracking may be viewed as proceeding via catalytic cycles in which surface carbenium ions are formed, participate in a series of reactions producing new surface and gas phase species, and terminate by desorption as olefins. The activity and selectivity of a catalyst are related to the relative rates of different catalytic cycles. Thus, while the nature of catalytic cycles may not change from one catalyst to another, the activity and selectivity may change based on how individual cycles are affected by catalyst properties or reaction conditions.

Figures 4a and 4b show schematic diagrams of catalytic cycles that are important at the entrance and the exit of the reactor, respectively. Table 1 lists the forward and net rates of the individual reactions of these catalytic

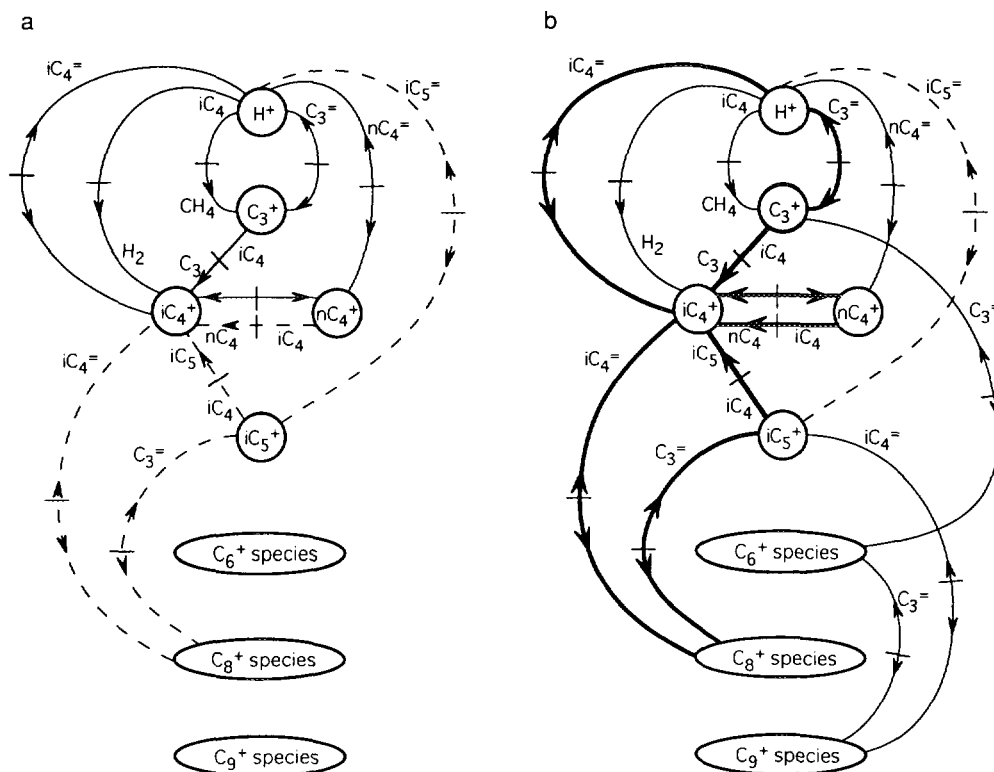


FIG. 4. Catalytic cycles for isobutane cracking over USY-C at 773 K and 11% conversion for a position in a plug-flow reactor that is at (a) 5% of reactor length and (b) the reactor exit.

cycles for isobutane cracking over USY-C at 11% conversion. Catalytic cycles are derived from these diagrams by starting at a surface species and following reaction lines connecting various surface species until returning to the original surface species. Each line connecting surface species is divided into two regions by an intersecting line segment. Gaseous reactants are written next to the reaction line connected to the corresponding surface reactant. Depending on where the gaseous species are written relative to the intersecting line segment, they may be products or reactants. The dashed reaction lines indicate the slowest processes, and the thickness of solid reaction lines indicate the relative rates of the faster processes. The arrows associated with the intersecting line segments indicate directions of allowed reaction pathways. A single arrow indicates an irreversible process, arrows of equal length indicate an equilibrated process, and arrows of unequal length indicate a reversible step with a faster rate in one direction. A particular reaction step may be part of more than one catalytic cycle. Therefore, when one constructs a catalytic cycle, the net rate indicated on one reaction line of the cycle may not necessarily be equal to the net rate indicated on another reaction line of the same cycle. *However, the steady state approximation for each surface species is always valid. Specifically, the net rate*

of production of a particular surface species by all reaction lines connected to that species is equal to the net rate of consumption of that surface species.

Catalytic cycles, as shown in Figs. 4a and 4b, allow us to rationalize and explain observed product selectivities. For example, initiation/desorption cycles include initiation reactions followed by olefin desorption and lead to the production of olefins. Olefins are also produced by oligomerization/ β -scission cycles that include the formation of surface carbenium ions, followed by a series of oligomerization and β -scission steps before the deprotonation and desorption of the resulting carbenium ion. Hydride ion transfer cycles start with the formation of a surface carbenium ion that abstracts a hydride ion from isobutane, forming a gas phase paraffin and a surface isobutyl cation. This cation can isomerize and/or transfer a proton to the surface and desorb as a C_4 olefin. Isopentane is produced by a variation of this cycle that includes oligomerization and β -scission steps. The net result of hydride ion transfer cycles is the production of paraffins.

At the entrance of the reactor where the conversion is small, many reaction pathways are too slow to be included in Fig. 4a. Under these conditions, initiation, olefin desorption, and isomerization are the dominant reaction pathways. The catalytic cycles at the reactor entrance are

mainly initiation/desorption cycles and the hydride ion transfer cycle producing propane. These cycles lead to C_3 and C_4 olefins as the preferred products. *The overall activity is equal to the total rates of initiation and hydride ion transfer reactions involving isobutane.*

Cycles describing the reactions at the bed exit are shown in Fig. 4b. As conversion increases and coverages of surface carbenium ions increase, reactions such as hydride ion transfer and oligomerization become important. In addition, β -scission reactions that are insignificant at the entrance of the reactor become important as coverages of larger surface species increase via oligomerization reactions. These changes result in lower olefin selectivity. For example, the paraffin to olefin ratio close to the bed entrance is 0.04 corresponding to a low isobutane conversion of 0.05%, while at the bed exit and a conversion of 11% this ratio is 2.6.

As conversion increases, the importance of different catalytic cycles for production or consumption of a particular species may vary. Consider the various catalytic cycles that produce and consume propylene. An initiation/desorption cycle yields propylene, in which isobutane reacts with a surface proton at low conversions to produce methane and a C_3^+ intermediate. This carbenium ion subsequently transfers a proton to the surface yielding propylene and thereby closing the cycle. However, at 773 K and ca. 2% conversion, the net reaction rate for propylene desorption is reversed, and this reaction consumes propylene. Under these conditions, other catalytic cycles become dominant. For example, in the hydride ion transfer cycle yielding propane, propylene adsorbs on a Brønsted acid site to form a propyl carbenium ion, followed by hydride ion transfer from an isobutane molecule to form propane and an isobutyl cation which decomposes to isobutylene and a surface proton. Alternatively, the cycle may be closed by isomerization of the isobutyl cation to an n -butyl cation that desorbs as a normal olefin. Propylene is also produced in an oligomerization/ β -scission cycle. An isobutyl cation formed by initiation or olefin adsorption reacts with isobutylene to form C_8^+ intermediates that subsequently undergo β -scission to yield propylene. The resulting isopentyl cation reacts with isobutylene to give C_9^+ intermediates that undergo two β -scission reactions to produce propylene and a propyl cation. The cycle closes with the propyl cation transferring a proton to the surface and desorbing as propylene. Since this cycle produces four propylene molecules for every three isobutylene molecules it consumes, the net result of this cycle is to produce olefins in excess of the amounts produced by the initiation/desorption cycles. This result does not change when the isobutylene adsorption and propylene desorption sections of this cycle are dominated by other cycles, because the rest of this cycle still produces more olefins than it consumes. For isobutane crack-

ing on USY-C at 773 K, the initiation/desorption cycle accounts for 99% of propylene produced at a conversion of ca. 0.2%. However, at the exit of the reactor at a conversion of ca. 11%, the hydride ion transfer cycle consumes all the propylene produced by the initiation/desorption cycle and about 70% of the propylene produced by the oligomerization/ β -scission cycle, and hydride ion transfer replaces propylene with propane and C_4 olefins.

Isobutylene is another species that participates in different catalytic cycles. For example, the initiation/desorption cycle involves isobutane protolysis to form hydrogen and an isobutyl cation followed by its deprotonation and desorption as isobutylene. The latter is also formed by hydride ion transfer cycles which are terminated by the same deprotonation reaction. In addition, isobutylene is consumed in the oligomerization/ β -scission cycle. Oligomerization/ β -scission reactions account for the consumption of about 2% of isobutylene produced by deprotonation and desorption of the isobutyl cation at a conversion of ca. 0.2%. As the conversion approaches 11% at the exit of the reactor, the percentage, in terms of reaction TOF's, of isobutylene consumed via this route increases to about 90%.

Role of Reactions in Product Selectivity

As discussed above, the observed activity and selectivity depend on the rates of the catalytic cycles which in turn are influenced by conversion, temperature, and acid strength. Table 2 lists the net rates of all reaction steps for USY-C at 773 and 733 K and for USY-S at 773 K. Figure 5, for example, shows how the combined rates of the important processes change with reactor length (or conversion) for catalyst USY-C. This figure illustrates the autocatalytic nature of catalytic cracking. Initiation/desorption and hydride ion transfer cycles that consume isobutane determine catalytic activity. As shown in Fig. 5, initiation is the dominant reaction at the reactor entrance. As conversion increases, the resulting increase in

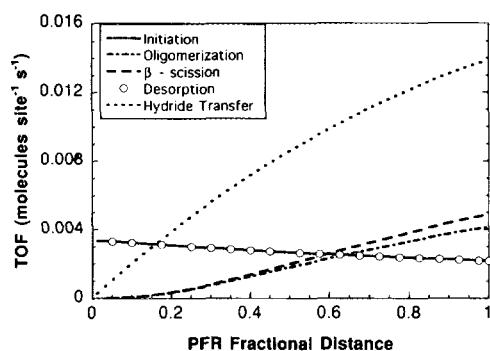


FIG. 5. Turnover frequencies with respect to reactor length for isobutane cracking over catalyst USY-C at 773 K and 11% conversion.

TABLE 4
Effects of Temperature and Catalyst Steaming on Reaction Rates

Reaction	Relative Rates	
	Temperature (USY-C, 733 K, 125 kPa)	Steaming (USY-S, 773 K, 137 kPa)
Initiation	0.2	0.5–0.6
Hydride ion transfer	0.35–0.5	0.25–0.35
Oligomerization/ β -scission	0.35–0.7	0.28–0.37

Note. Rates are relative to USY-C at 773 K and 152 kPa. Conversion equal to 10–12%.

carbenium ion coverages causes the rates of hydride ion transfer and therefore the rates of the corresponding cycles to increase. At high conversions, catalytic activity is mostly a function of hydride ion transfer processes. When the catalyst is steamed or the temperature is decreased, the rates of all reactions are reduced. Table 4 summarizes this reduction in the combined rates of the most important processes for both cases. Decreases in the rates of cycles that include initiation and hydride ion transfer reactions explain the observed reduction in catalytic activity caused by steaming and by lower temperatures.

Initiation reactions. Although the nature of initiation reactions cannot be determined in this study (10), we have assumed hydrogen formation via C–H bond protolysis and methane formation via C–C bond protolysis to be the two initiation reactions. These reactions are irreversible. Since these reactions require a proton to attack the alkane, we expect the rates of these steps to decrease with steaming because steaming reduces the Brønsted acid strength of the catalyst. Indeed, activation energies of initiation reactions appear to increase with steaming (10), resulting in a decrease in turnover frequencies by a factor of 2 (Table 4). For the calcined catalyst the rate of C–C protolysis is 1.7 times faster than the rate of C–H protolysis, whereas these rates are almost equal for the steamed catalyst. Thus, our analysis suggests that the breaking of the C–C bond is more sensitive to changes in acid strength than the breaking of the C–H bond.

Changes in reaction temperature affect the rates in general by changing rate constants and surface coverages of carbenium ion intermediates. Initiation reactions rates, which are not a strong function of carbenium ion coverages, are affected almost exclusively by the temperature dependence of the rate constants. Activation energies are high, about 38 to 40 kcal/mol (10). A decrease in temperature by 40 K at constant conversion results in a decrease in the rates of initiation reactions by a factor of 5 (Table 4).

Hydride ion transfer reactions. Hydride ion transfer reactions determine the rate of paraffin formation. The

rates of these processes depend on the carbenium ion coverages, and their importance increases with surface coverage (Fig. 5). These reactions are irreversible (with the possible exception of the step which leads to isopentane formation) because of the positive enthalpy change associated with the formation of a secondary carbenium ion from a tertiary ion and the low pressures of gaseous species other than isobutane. The forward activation energies for the steps that lead to the formation of propane, butane, and isopentane were 17, 16, and 30 kcal/mol, respectively, for USY-C (10). The hydride ion transfer reaction producing isopentane seems to be the most difficult reaction. We speculate that increasing the size of the molecule reacting in the hydride ion transfer process affects the facility with which the reaction can proceed. Such behavior may be due to the requirement of bulky transition states which are sterically hindered within zeolite pores. Hydride ion transfer reactions are known to be hindered in small pore zeolites like ZSM-5 (16).

The decrease in Brønsted acid strength due to steaming results in decreasing the rates of hydride ion transfer reactions by as much as a factor of 4. This decrease in hydride ion transfer rates is larger than for initiation reactions and is due to the significantly lower fractional carbenium ion coverage on the steamed catalyst. This observation agrees with an earlier suggestion (17) that acid strength influences rates of hydride ion transfer reactions because strong Brønsted acidity is necessary to stabilize carbenium ions on the surface. It also explains data (1, 18) that indicate higher olefin selectivity on weak acid catalysts.

On the other hand, since activation energies for hydride ion transfer reactions (10) are lower than for initiation reactions, and since tertiary carbenium ion coverage increases at lower temperature, rates of hydride ion transfer reactions decrease to a lesser extent than initiation reaction rates with decreasing temperature. For a decrease in temperature by 40 K, the rates of the hydride ion transfer reactions decrease by a factor of 2–3 depending on conversion.

Oligomerization/ β -scission reactions. Oligomerization/ β -scission reactions are reversible. Their rates are a

function of the carbenium ion coverages and the partial pressures of the gas phase olefins. Hence, both components are required in substantial amounts before these reactions can proceed at appreciable rates. As shown in Fig. 5, the rates of these reactions do not increase as rapidly with conversion as the rates of hydride ion transfer reactions. Lowering the Brønsted acid strength of the catalyst lowers the rates of oligomerization/ β -scission reactions. The reaction rates estimated for USY-S are lower by a factor of 3 (Table 4) compared to USY-C.

The effects of temperature on the rates of oligomerization/ β -scission reactions are similar to the effects on hydride ion transfer reactions. A decrease in temperature by 40 K results in a decrease in the rates of oligomerization/ β -scission reactions by a factor of 1.5–3, depending on conversion. Oligomerization processes generally have higher activation energies than hydride ion transfer reactions (10). However, they involve surface tertiary carbenium ions only, as well as gas phase olefins; surface coverages of the former species increase at lower temperatures, while partial pressures of olefins in the product stream decrease at lower temperatures.

The net rate of β -scission reactions is higher than the net rate of oligomerization reactions. This difference, which increases with increasing conversion, is equal to the rate of formation of olefins by the oligomerization/ β -scission cycle: the only route that leads to net olefin production other than via initiation/desorption cycles. Figure 6 shows the contribution of the oligomerization/ β -scission cycle to total olefin production versus reactor length (or conversion). The oligomerization/ β -scission cycle contributes substantially to olefin formation only at high conversions. At constant conversion, this contribution to olefin formation decreases with steaming and increases at lower temperature. For the weaker acid catalyst USY-S, the lower carbenium ion coverages result in lowering the rates of

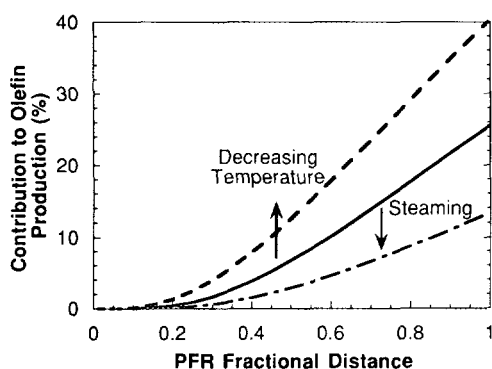


FIG. 6. Percent contribution of the oligomerization/ β -scission cycle to the TOF of the total olefin production during isobutane cracking on USY-C catalyst at 773 K (—), 733 K (---), and on catalyst USY-S at 773 K (-·-).

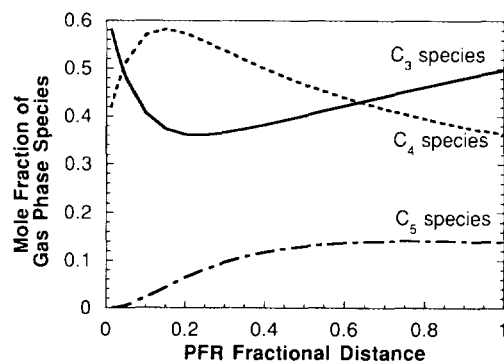


FIG. 7. Changes in the distribution of C_3 (—), C_4 (---), and C_5 (-·-) species with reactor length for catalyst USY-C at 773 K and 40.5% conversion. Values in mole fraction of the total amount of C_3 , C_4 , and C_5 species in the gas phase.

the oligomerization/ β -scission reactions to a greater extent than initiation reactions. The opposite is true at lower temperatures, since the rates of the oligomerization/ β -scission reactions are less sensitive to temperature than initiation reactions.

The oligomerization/ β -scission cycle also changes the carbon distribution among product hydrocarbons by consuming C_4 and producing C_3 and C_5 hydrocarbons (Fig. 7). The product is rich in C_3 at the reactor inlet. As conversion increases, C_3 selectivity decreases and goes through a minimum while C_4 selectivity increases and goes through a maximum. C_5 hydrocarbons increase gradually with conversion. Changes in selectivity may be discussed in four stages. The initiation/desorption cycles dominate the selectivity at very low conversions. As conversion increases, hydride ion transfer cycles increase selectivity of C_4 hydrocarbons. At even higher conversions, the oligomerization/ β -scission cycle consumes C_4 hydrocarbons and forms C_3 and C_5 hydrocarbons. Finally, oligomerization of isopentyl cations with isobutylene leads to the formation of C_3 while reducing C_4 and C_5 hydrocarbons. This behavior agrees with the experimentally observed increase in C_3 selectivity at the expense of C_4 for conversions above 10% (10).

The same interplay of catalytic cycles controls product selectivity at different acid strengths and temperatures. Lowering Brønsted acid strength via steaming decreases the role of coverage dependent catalytic cycles and the C–C bond protolysis rate. The latter effect results in lower initial C_3 selectivity. Lower temperatures, on the other hand, increase the role of coverage dependent processes, particularly those of hydride ion transfer reactions. The decrease in C_3 selectivity due to the enhanced role of hydride ion transfer reactions cannot be compensated for by the oligomerization/ β -scission reaction cycle. Therefore, C_3 concentration in the product stream should de-

crease with temperature at constant conversion. This agrees with experimental data: at 10–11% conversion, a 40 K temperature decrease results in a C_3 selectivity decrease from 37 to 32%.

Olefin desorption and isomerization reactions. Olefin desorption reactions are in quasi-equilibrium, and since these reactions follow the initiation reactions to complete the formation of olefins by the initiation/desorption cycles, the net rates of these steps are equal to those of the initiation reactions (Fig. 5). The olefin desorption reactions essentially determine the surface carbenium ion coverages. Thus, even though by themselves they are kinetically insignificant, and do not influence the overall reaction rate, they have a significant impact on the rates of hydride ion transfer, oligomerization, and β -scission reactions. When catalyst steaming increases the value of ΔH_{ads} , the desorption equilibrium constants increase and olefin desorption is favored. This reduces the surface coverage by carbenium ions (Table 3). But, when temperature is decreased, the equilibrium shift favors olefin adsorption which results in higher surface coverages. Thus, decreasing temperature or Brønsted acid strength has opposite effects on carbenium ion coverage.

Isomerization reactions are also in quasi-equilibrium and determine the relative amounts of the various isomeric carbenium ions. Steaming the catalyst does not affect the isomerization equilibrium constant, since the equilibrium constant is not a function of acid strength. Lower temperature, however, by shifting the equilibrium, favors tertiary over secondary carbenium ions and the relative amount of tertiary versus secondary carbenium ions increases.

Methide transfer reaction. An important attribute of microkinetic modeling is the ability to add steps to a mechanism in order to ascertain their importance or relevance. Isopentane formation in our model occurs via hydride ion transfer to a tertiary isopentyl carbenium ion. Recently it was suggested (19) that a methide transfer step between isobutane and n -butyl cations should be considered for isopentane formation. We, therefore, introduced the following step in our reaction network and repeated the fitting procedure for USY-C:



The kinetic model gives good fits of the data with or without this methide transfer step; therefore we cannot ascertain if such a step is important. However, if this step does occur, our analysis indicates that it will contribute to isopentane formation only at the reactor entrance or at very low conversions (<0.5%), i.e., when the surface coverage of isopentyl carbenium ions is negligibly small,

and little isopentane is produced by hydride ion transfer. As coverage of isopentyl carbenium ions increases, the hydride ion transfer reaction rapidly becomes dominant.

Paraffin–Olefin Selectivity

Changes in the rates of catalytic cycles result in changing paraffin and olefin selectivity. Carbon and hydrogen balances close when all organic species are counted, and there is no net influx of hydrogen in the products (20, 21). The paraffin to olefin ratio depends on how one counts the paraffins and olefins. If a reactant paraffin cracks into one paraffin and one olefin, then one product paraffin is counted for every product olefin, giving a paraffin to olefin ratio of 1 : 1. However, if a product olefin cracks further into two smaller product olefins, then an additional olefin is counted in the products. If a reactant paraffin reacts with a product olefin to give a product paraffin and another product olefin, or if a reactant paraffin isomerizes to a product paraffin, then a net product paraffin is counted. Thus it is possible to observe paraffin to olefin ratios with values greater or smaller than 1.

Initiation reactions produce hydrogen, methane, propylene, and isobutylene. Ethylene is formed by a separate process not involving carbenium ions. Coke formation is not taken into account by our model. We define the paraffin to olefin ratio in terms of C_n species for $n \geq 3$. Our analysis of catalytic cycles that lead to paraffin and olefin formation indicates that *the rate of paraffin production versus the rate of olefin production at any point inside the reactor is equal to the ratio of the rates of hydride ion transfer reactions to the rates of all initiation reactions plus the net rate of olefin production from the oligomerization/ β -scission cycle.* This ratio of rates will be written as $R_{C_n}/R_{C_n}^-$ ($n \geq 3$), where R_i represents the TOF for the production of species i in units of molecules site⁻¹ s⁻¹.

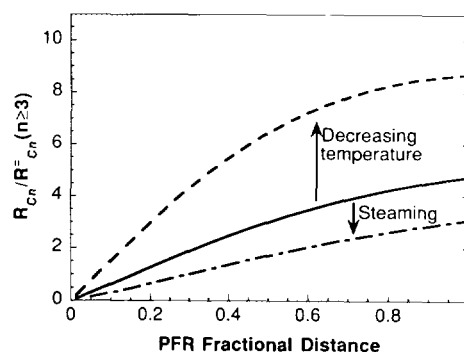


FIG. 8. Ratio of paraffin production rate to olefin production rate at different reactor lengths for USY-C at 773 K and 11% conversion (—), USY-C at 773 K and 12% conversion (---), and USY-S at 773 K and 10% conversion (-·-). Areas under the curve represent the paraffin to olefin ratio, equal to 2.6, 5.3, and 1.6 respectively, measured at the exit of the reactor.

Figure 8 shows how $R_{C_n}/R_{C_n}^-$ ($n \geq 3$) changes with reactor length (or conversion), temperature, and steaming. This ratio increases with increasing conversion and decreasing temperature, whereas it decreases with steaming. The rates of initiation reactions do not change significantly with increasing conversion or reactor length, whereas the rates of hydride ion transfer, oligomerization, and β -scission reactions increase substantially. Therefore, hydride ion transfer cycles that produce paraffins are favored when conversion increases, and the $R_{C_n}/R_{C_n}^-$ ($n \geq 3$) ratio initially increases with conversion (Fig. 8). At conversions higher than ca. 30%, the $R_{C_n}/R_{C_n}^-$ ($n \geq 3$) ratio decreases due to two factors. First, olefin formation via the oligomerization/ β -scission cycle increases due to an increase in the presence of C_4 olefins which are required for oligomerization. Second, lower isobutane pressure suppresses the rates of hydride ion transfer reactions.

When catalyst acid strength is decreased by steaming, the rates of all surface processes are reduced. However, due to lower carbenium ion coverages on the steamed catalyst, the rates of hydride ion transfer and oligomerization/ β -scission reactions decrease more than the rates of initiation reactions. Since initiation/desorption cycles that produce olefins are less affected by steaming, and since the contribution of the oligomerization/ β -scission reactions to olefin production is relatively low, the steamed catalyst exhibits the increased olefin selectivity shown in Fig. 8. Lower temperatures favor hydride ion transfer cycles more than initiation/desorption cycles, resulting in higher paraffin selectivities at lower temperatures. However, at higher conversions, since the oligomerization/ β -scission cycle is also favored at low temperatures, the $R_{C_n}/R_{C_n}^-$ ($n \geq 3$) ratio is reduced.

These conclusions agree with data reported elsewhere (1, 9, 14, 22–24) on the effects of conversion and temperature on paraffin to olefin ratios. Our observation that the paraffin to olefin ratio decreases with increasing Si/Al ratio for paraffin cracking over Y zeolites concurs with the results in Refs. (23, 25, 26) but not with Shertukde *et al.* (4). Recently Corma and co-workers (9) reported that during isobutane cracking at 773 K the catalyst with higher Si/Al ratio had a lower paraffin selectivity, but that this trend was reversed at 673 K. Our model can explain this reversal in paraffin selectivity. With increased steaming severity, hydride ion transfer reaction rates decrease to a greater extent than initiation reaction rates. Therefore, the latter reactions are more important for controlling product selectivity on steamed catalysts with high Si/Al ratios. But decreasing reaction temperature affects initiation rates more severely than hydride ion transfer rates. Due to such a severe temperature effect on initiation rates and the increase in the activation energies of these reactions with steaming, initiation reactions on a more severely steamed catalyst will be affected to a greater extent

than on a less severely steamed catalyst at lower reaction temperatures. Since hydride ion transfer rates are not lowered to the same extent as initiation rates with temperature, this will result in progressively higher paraffin/olefin ratios for steamed catalysts as reaction temperatures are lowered, with the greatest effect on the more severely steamed catalyst, leading to the observed trend in Ref. (9).

SUMMARY AND CONCLUSIONS

Isobutane cracking and in general any catalytic cracking is described by catalytic cycles that involve carbenium ion initiation, β -scission, oligomerization, olefin desorption (proton transfer), isomerization, and hydride ion transfer reactions. Though the fundamental chemistry of catalytic cracking remains unchanged, different experimental conditions or changes in acid strength change the relative rates of these cycles and thus alter catalytic activity and selectivity. Individual surface reactions determine the rates of these catalytic cycles. Initiation reactions are irreversible, insensitive to conversion, and, in conjunction with olefin desorption reactions, form olefins. Hydride ion transfer reactions are also irreversible, lead to paraffin formation, and depend on carbenium ion surface coverages. Oligomerization and β -scission processes are reversible, and their rates depend on surface coverages and gas phase olefin pressures. Catalytic cycles involving oligomerization and β -scission produce olefins and impact the distribution of C_3 , C_4 , and C_5 products. Olefin adsorption/desorption reactions are in quasi-equilibrium, but by determining surface coverages of carbenium ions have a significant impact on activity and selectivity.

Since catalytic cracking proceeds via a number of different catalytic cycles, the concept of a single controlling step is not applicable. The importance of a cycle will depend on the experimental conditions or catalyst used. For example, at very high conversions the hydride ion transfer cycles are dominant enough to determine isobutane conversion, while initiation reactions will similarly dominate at the very early stages of the overall reaction. In fact, at 1% conversion (catalyst USY-C at 773 K) initiation/desorption cycles contribute only about 50% of the total activity (in terms of the turnover frequency). This contribution initially drops rapidly with conversion and then decreases gradually to 7% at 40% conversion.

Using microcalorimetric measurements with ammonia, we found that steam treatment reduces the strength of Brønsted acid sites. Experimentally, this results in a lower site time yield of isobutane on the steamed catalyst. The model substantiates these experimental observations by increasing the adjustable parameter ΔH_+ , the difference in the heats of stabilization of a carbenium ion versus a proton on the surface, for the steamed catalyst. Although a decrease in acid strength with catalyst steaming de-

creases turnover frequencies of all reactions, the largest effect is on the rates of hydride ion transfer reactions. The decrease in the rates of hydride ion transfer reactions results primarily from the decrease in carbenium ion coverages. Initiation rates decrease because activation energies for these reactions become less favorable. The steamed catalyst, therefore, has a lower hydride ion transfer/initiation rate ratio than USY-C, which translates into lower paraffin/olefin ratios.

Our model explains why catalysts with lower Brønsted acid strength have lower coverage of surface carbenium ions. The latter are in quasi-equilibrium with gas phase olefins. This does not mean that steaming decreases the pressures of olefins. The decrease in coverage is because a decrease in acid strength alters the equilibrium constants of olefin desorption, making olefin desorption thermodynamically more favorable. Thus lower carbenium ion coverages can be maintained at higher olefin pressures.

Temperature changes affect initiation reactions which have higher activation energies than hydride ion transfer reactions. Decreasing temperature results in increased surface carbenium ion coverage and increased paraffin to olefin selectivity. The increased coverage is again due to the shift in the olefin-surface carbenium ion equilibrium which at lower temperatures favors higher surface coverages. Thus a quasi-equilibrium step, which may often be dismissed as being kinetically insignificant, plays an important role in catalytic cracking. It determines surface coverages of carbenium ion intermediates as catalyst acid strength or reaction conditions change and thus directly influences the rates of other reactions and cycles.

ACKNOWLEDGMENTS

We thank Stan Koziol for carrying out the kinetic measurements and Gail Hodge for the FTIR work. This work was partially supported by funds provided by Engelhard Corp. and the Office of Basic Energy Sciences of the U.S. Department of Energy (DE-FG02-84ER13183). This work was also supported in part by the U.S. Environmental Protection Agency and the Center for Clean Industrial and Treatment Technologies.

REFERENCES

1. McVicker, G. B., Kramer, G. M., and Ziemiak, J. J., *J. Catal.* **83**, 286 (1983).
2. Lombardo, E. A., Pierantozzi, R., and Hall, W. K., *J. Catal.* **104**, 171 (1988).
3. Lombardo, E. A., and Hall, W. K., *J. Catal.* **112**, 565 (1988).
4. Shertukde, P. V., Marcelin, G., Sill, G. A., and Hall, W. K., *J. Catal.* **136**, 446 (1992).
5. Zhao, Y., Bamwenda, G. R., Groten, W. A., and Wojciechowski, B. W., *J. Catal.* **140**, 243 (1993).
6. Stefanadis, C., Gates, B. C., and Haag, W. O., *J. Molec. Catal.* **67**, 363 (1991).
7. Krannila, H., Haag, W. O., and Gates, B. C., *J. Catal.* **135**, 115 (1992).
8. Rekoske, J. E., Madon, R. J., Aparicio, L. M., and Dumesic, J. A., in "Proceedings, 10th International Congress on Catalysis, Budapest, July 1992," (L. Gucci *et al.*, Eds.) p. 1653. Elsevier, Amsterdam, 1993.
9. Corma, A., Miguel, P. J., and Orchilles, A. V., *J. Catal.* **145**, 171 (1994).
10. Yaluri, G., Rekoske, J. E., Aparicio, L. M., Madon, R. J., and Dumesic, J. A., **153**, 54 (1995).
11. Handy, B. E., Sharma, S. B., Spiewak, B. E., and Dumesic, J. A., *Meas. Sci. Technol.* **4**, 1350 (1993).
12. Cardona-Martinez, N., and Dumesic, J. A., *J. Catal.* **125**, 427 (1990).
13. Chen, D., Sharma, S., Cardona-Martínez, N., Dumesic, J. A., Bell, V. A., Hodge, G. D., and Madon, R. J., *J. Catal.* **136**, 392 (1992).
14. Kogelbauer, A., and Lercher, J. A., *J. Catal.* **125**, 197 (1990).
15. Engelhardt, J., and Hall, W. K., *J. Catal.* **125**, 472 (1990).
16. Haag, W. O., Lago, R. M., and Weisz, P. B., *Discuss. Faraday Soc.* **72**, 317 (1981).
17. Madon, R. J., *J. Catal.* **129**, 275 (1991).
18. Haag, W. O., and Dessau, R. M., in "Proceedings, 8th International Congress on Catalysis, Berlin, 1984," Vol. 2, p. 305.
19. Hall, W. K., private communication.
20. Abbot, J., and Wojciechowski, B. W., *J. Catal.* **109**, 274 (1988).
21. Abbot, J., and Wojciechowski, B. W., *J. Catal.* **107**, 451 (1987).
22. Abbot, J., and Wojciechowski, B. W., *J. Catal.* **113**, 353 (1988).
23. Corma, A., and Orchillés, A. V., *J. Catal.* **115**, 551 (1989).
24. Shigeishi, R., Garforth, A., Harris, I., and Dwyer, J., *J. Catal.* **130**, 423 (1991).
25. Wang, Q. L., Giannetto, G., and Guisnet, M., *J. Catal.* **130**, 471 (1991).
26. Wielers, A. F. H., Vaarkamp, M., and Post, M. F. M., *J. Catal.* **127**, 51 (1991).